Meat Science xxx (xxxx) xxxx

Contents lists available at ScienceDirect

Meat Science

journal homepage: www.elsevier.com/locate/meatsci

A modified nanocomposite biosensor for quantitative L-glutamate detection in beef

Xiaodan Wang[a,*], Jinjiao Duan[a], Yingming Cai[a], Dengyong Liu[b,**], Xing Li[a], Yanli Dong[a], Feng Hu[a]

[a] College of Food Science and Engineering, Jilin University, Changchun 130062, China
[b] College of Food Science and Technology, Bohai University, Jinzhou 121013, China

ARTICLE INFO

Keywords:
Beef
L-Glutamate
Biosensor
Quantitative detection
Glutamate oxidase

ABSTRACT

A new biosensor for detecting L-glutamate (L-Glu) in beef was developed. Firstly, a bare Au electrode was surface-modified by gold nanoparticles (Au NPs), graphene oxide (GO), and chitosan (CS) as immobilized materials, and then its surface was connected with L-glutamate oxidase (GluOx). The modified Au NPs/GO/CS electrode was characterized by scanning electron microscopy, and the formation mechanism was elaborated. The response current of the L-Glu biosensor maximized to 0.08 mA at pH 7.5 and 0.09 mA at 30 °C, with a detection range of 0.2–1.4 mM and a detection limit of 0.023 mM. The L-Glu biosensor had high accuracy, and its results linearly fitted with those of the amino acid analyzer with a coefficient of 0.996. The L-Glu biosensor had high selectivity, repeatability, and stability and detected higher L-Glu content in the cooked beef than in the raw beef.

1. Introduction

In modern society, the global demand for consumption of healthier meat products is rising (Scollan et al., 2014). Beef products as a rich source of proteins and other nutrients are both nutritious and delicious. Beef quality is mainly decided by flavor, juiciness, and tenderness, which also highly influence the decision-making of consumers on repeated purchase (Hocquette et al., 2012). Particularly, flavor considerably impacts the commercial and edible values of beef. Amino acids are not only one of the main sources of meat flavor, but also can be used as common nutrients. In meat, L-glutamate (L-Glu) has strong flavor enhancement effect and has the delicate flavor and characteristics of improving flavor (Hayashi, Yamaguchi, & Konosu, 1981).

The existing L-Glu detection methods mainly include high-performance liquid chromatography, gas chromatography–mass spectrometry (Buck, Voehringer, & Ferger, 2009; Clarke, O'Mahony, Malone, & Dinan, 2007), fluorimetry (Tadayuki & Kiyoshi, 2005), and spectrophotometry (Acebal, Lista, & Fernández Band, 2008; Khampha, Meevootisom, & Wiyakrutta, 2004; Tang, Zhu, Xu, Yang, & Li, 2007), but these methods are limited by the requirement for expensive equipment and professional technical staff as well as complex operation. Biosensors are considered as one of the most potential approach, because of the high sensitivity, rapidity, easy detection, convenience, and wide detection range(Chuanrui, Yue, Peining, & Huisheng, 2020; Shen & Burgess, 2018). The application of biosensors in food industry mainly includes food composition analysis, food quality, and safety detection (Omanovic-Miklicanin & Valzacchi, 2017; Stredansky, Redivo, Magdolen, Stredansky, & Navarini, 2018). Biosensors were used to detect L-Glu contents in human serum, tomatoes, and noodle soups (Batra, Yadav, & Pundir, 2016). A modified screen-printed electrode was used to detect L-Glu in monosodium and human serum (Hughes, Pemberton, Fielden, & Hart, 2015). A biosensor was fabricated by coating CHIT–CNT–AuNW on the electrode surface to measure L-Glu in foods (Kitikul, Satienperakul, Preechaworapun, Pookmanee, & Tangkuaram, 2017). An L-Glu biosensor was successfully applied to determine monosodium glutamate in soy sauce and tomato sauce (Basu, Chattopadhyay, Roychudhuri, & Chakraborty, 2006).

In recent years, nanoparticles have received considerable attention because of their high catalysis and biocompatibility (Upadhyay et al., 2009). Biosensors based on the nanocomposite-modified electrode are a current research hotspot. Au nanoparticles have been widely studied owing to the high biocompatibility, large specific surface area, high electrical conductivity (Cao et al., 2010), simple preparation method, and controllable particle size. Graphene oxide (GO), a new material,

* Corresponding author at: College of Food Science and Engineering, Jilin University, No. 5333, Xi'an Road, Changchun, Jilin, China.
** Corresponding author at: College of Food Science and Technology, Bohai University, No. 19, Keji Road, New Songshan District, Jinzhou City, Liaoning Province, China.
E-mail addresses: jxd@jlu.edu.cn (X. Wang), jz_dyliu@126.com (D. Liu).

https://doi.org/10.1016/j.meatsci.2020.108185
Received 6 July 2019; Received in revised form 29 March 2020

contains abundant surface functional groups such as hydroxy group and epoxy group. GO is a highly desirable material that outperforms other nanomaterials in terms of excellent electric conductivity, biocompatibilty, unusual electrical and chemical properties, high thermal stability, high mechanical strength, and water solubility (Elancheziyan, Manoj, Saravanakumar, Thenmozhi, & Senthilkumar, 2017; Kuila et al., 2011; Song et al., 2013). For these reasons, GO has unique advantages in functional graphene materials and the preparation of high-performance composites. GO has been widely used in electrochemical fields (Ali, Hwang, Choo, & Dong, 2017). Chitosan (CS), also known as deacetyl chitin, has many excellent properties in physical, chemical, and biological properties. CS is rich in amino groups and has high biocompatibility, nontoxicity, and favorable film-forming properties (Denuziere, Ferrier, Damour, & Domard, 1998; Shi & Ma, 2010; Sorlier, Denuzière, Viton, & Domard, 2001).

This study is aimed to use biosensors to detect L-Glu in beef. The gold electrode was surface-modified by using an L-glutamate oxidase (GluOx)/gold nanoparticles (Au NPs)/GO/CS suspension. This is the first report about the fabrication of an amperometric sensor using the Au electrode modified with GluOx/Au NPs/GO/CS and its application to construct an amperometric biosensor for L-Glu detection in beef. The new biosensor is expected to provide high stability, biocompatibility, repeatability, and sensitivity.

2. Experimental

2.1. Reagents and materials

The reagents used here included GluOx (from Streptomyces, ≥5.0 U/mg, Sigma–Aldrich, China), gold (III) chloride tetrahydrate ($HAuCl_4 \cdot 3H_2O$, Sangon Biotech Co. Ltd., Shanghai, China), chitosan, L-Glu (Shanghai Sinopharm Chemical Reagent Co. Ltd., China), graphite (99%, Nanjing Xianfeng Nanomaterials Technology Co. Ltd., China); N-ethyl-N´-(3-dimethylaminopropyl) carbodiimide (EDC) and N-hydroxy succinimide (NHS) (Shanghai Source Leaf Biotechnology Co. Ltd.). Phosphate buffer solutions (PBS) at different pH levels were prepared from analytical-grade chemicals and used without further purification. All of the solutions were prepared in double-distilled water (DW).

2.2. Apparatuses

The samples were first characterized on CHI660D electrochemical analysis system (Chenhua, Shanghai, China). A conventional three-electrode system involving a Au electrode (diameter = 2 mm) as the working electrode, Pt wire as the auxiliary electrode, and the reference Ag/AgCl electrode was used. Other apparatuses included an XL-30 scanning electron microscope (SEM, FEI Co.), an IRPRESTIGE-21 Fourier transform infrared spectrometer (FTIR, SHIMADZU, Japan), a D8 ADVANCE X-ray diffractometer (XRD, BRUKER Co. Germany), a meat grinder (HansJiaOurs Co, Germany), a magnetic heating agitator (Shanghai Instrument Electric Science Instrument Ltd., China), and an L8900 amino acid auto-analyzer (Hitachi Co. Ltd., Japan).

2.3. Beef sample preparation

The cattle (Jilin Changchun Haoyue Group Co. Ltd. Jilin Province, China) aged 30–36 months and weighed 400–550 kg were selected. After slaughtering according to the standard, the beef was cooled at 4 °C for 48 h and then segmented. After that, the longissimus thoracis were transported to the laboratory with vacuum packing at 4 °C and used to detect the test samples. The connective tissues of the samples were removed. The beef samples were cut into small pieces of $10 \times 10 \times 10$ mm^3, and a small meat grinder was used to separate the uniform minced meat. The minced meat samples were divided into two groups, each weighing 20 g (Han et al., 2017).

The first group was named C_{cooked} for analysis of amino acid content in cooked beef. The samples were placed in a water bath, heated at 80 °C for 20 min, and then cooled to room temperature (RT). The second group was named C_{raw} for analysis of amino acid content in raw beef. All experiments were conducted in triplicate and at RT (20 ± 2 °C).

The two groups (raw and cooked) of meat samples were prepared according to GB 5009.124-2016 (Zhang et al., 2017) and stored at 4 °C for testing. Firstly, all meat samples of the two groups were weighed (1 ± 0.001 g) and put into hydrolysis tubes separately. Secondly, the hydrolysis tubes were added with 10 mL of 6 mM hydrochloric acid solution and 0.1 g of reevaporate phenol, and four hydrolytic tubes were put into a refrigerant (salt mixed with ice in quality of 1:3) for 5 min. Then the tubes were vacuumized by a vacuum pump. When it was close to 0 Pa, high-purity nitrogen was introduced into the tubes and this step was repeated three times. Finally, under the condition of nitrogen filling, the screw cap was tightened and put in the electric heating oven constantly at 110 °C followed by hydrolysis for 22 h. Then the hydrolyzed meat samples were cooled to RT and filtered, and the filtered hydrolysates were filled with a 50 mL volumetric flask. The deionized water was repeatedly used to wash the tubes. The cleaning solution was also transferred to a 50 mL volumetric flask and used again. The deionized water was set to the mark and shaken.

2.4. Preparation of the L-Glu biosensor

2.4.1. Preparation of Au NPs/GO/CS suspension

First, graphite oxide was prepared via the improved Hummers method (Stankovich et al., 2007). Then GO was synthesized by ultrasonic stripping, which is the most general way to prepare GO from graphite oxide. Graphite oxide (10 mg) was dissolved in 10 mL of chitosan–acetic acid mixed solution to the concentration of 0.5%, stirred for 1.5 h at RT, and then treated for 2.5 h with the ultrasonic power of 90 W. With CS as a reducing agent, Au^{3+} was reduced to Au NPs at certain temperature. Therefore, the 0.5 mg/mL chloroauric acid solution (15 mL) was added to the chitosan–acetic acid mixed solution and stirred first at RT for 30 min and then at 80 °C for 1.5 h. Finally, the wine red suspension was preserved at 4 °C until use. The suspension can be dropped on the Au electrode.

2.4.2. Construction of the Au NPs/GO/CS modified Au electrode

Before modification, the surface of the Au electrode was polished before each experiment with 1, 0.3, or 0.05 μm alumina powder, then thoroughly washed with DW, placed into ethanol and DW for 1 min for sonication to remove absorbed particles, and finally dried with pure nitrogen. Then the Au NPs/GO/CS suspension (10 μL) was dropped on the surface of the Au electrode and dried at RT. The Au NPs/GO/CS modified electrode was placed in a mixed solution containing 0.2 M EDC and 0.05 M NHS for 30 min. Then the activated electrode was gently washed with a 0.01 M buffer solution (pH 7.5).

2.4.3. Immobilization of GluOx

The glutamate oxidase solution was prepared as follows: glutamate oxidase was dissolved in 0.01 mol/L PBS buffer solution at 30 °C, forming 0.05–0.1 unit/mL solutions. When glutamate oxidase freeze-dried powder was dissolved in PBS, the PBS can be precooled for 2–3 min at 4 °C. The prepared enzyme solution was generally frozen at −20 °C, but was unstable, so it should be used as soon as possible.

GluOx (4 μL, 0.008 U/μL) was dropped onto the surface of the Au NPs/GO/CS/Au to form GluOx/Au NPs/GO/CS/Au, and the enzyme-modified electrode was incubated overnight at 4 °C. The GluOx-immobilized electrode was washed gently with 0.01 M PBS (pH 7.5) to remove free enzymes. The L-Glu biosensor was characterized by SEM at different stages and stored at 4 °C until used. The fabrication process was shown in Fig. 1.

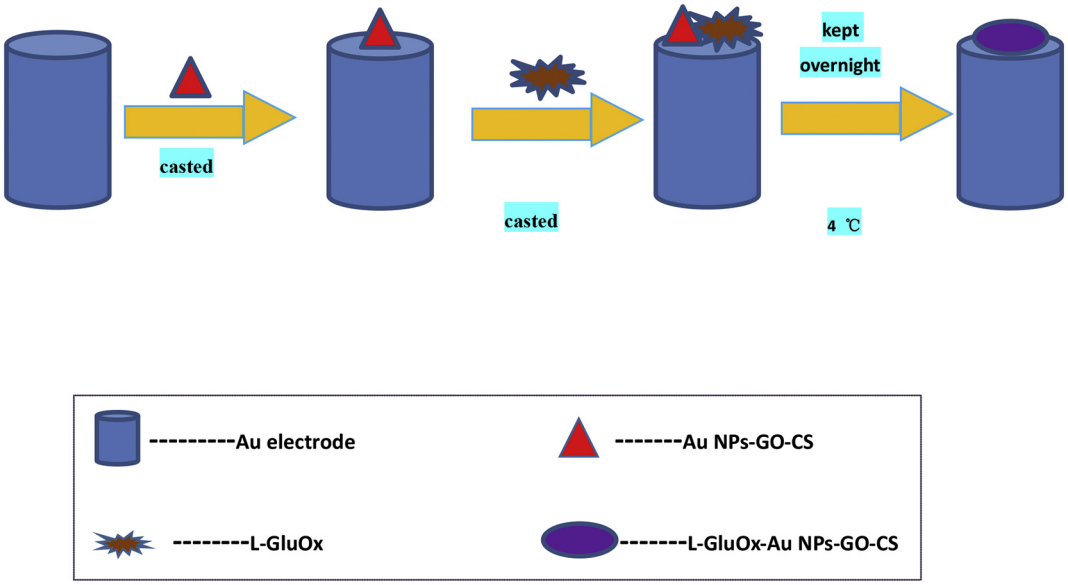

Fig. 1. Schematic diagram for the preparation of glutamate biosensor.

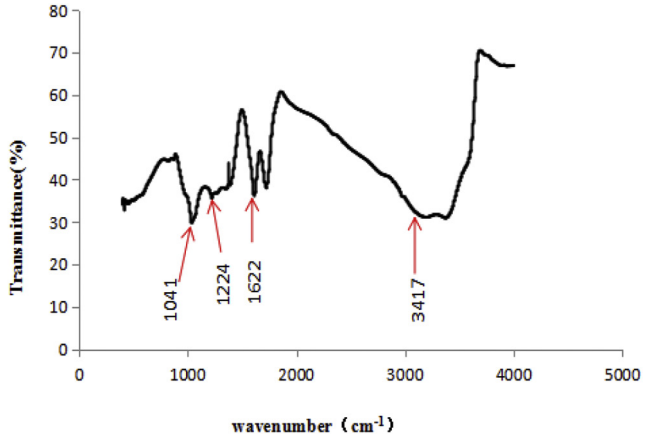

(a)

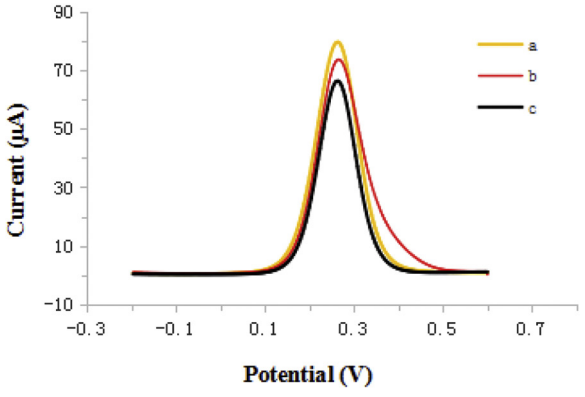

(a)

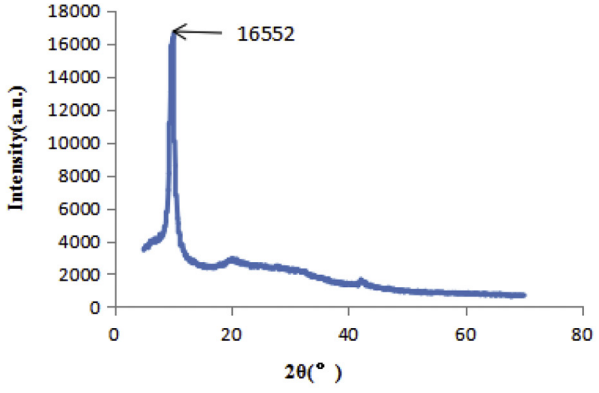

(b)

Fig. 2. (a) Infrared spectrum of GO; (b) XRD diagram of GO.

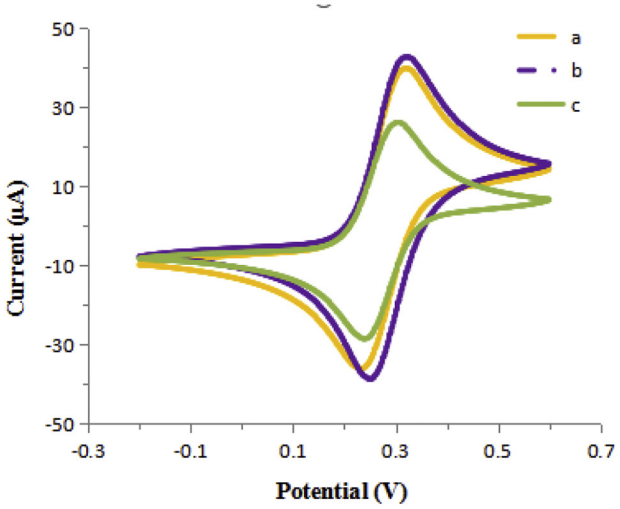

(b)

Fig. 3. (a) DPV and (b) CV of a – bare Au electrode, b – Au NPs/GO/CS modified electrode, c – Au NPs/GO/CS/L-GluOx electrode in the 0.1 mol/L PBS (pH = 7.5) containing L-Glu.

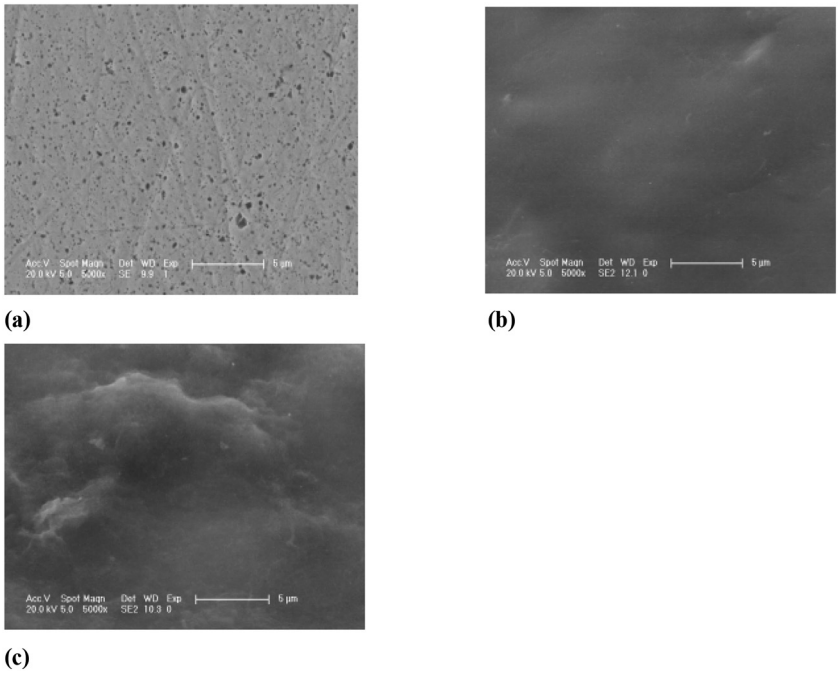

Fig. 4. (a) SEM image of bare Au electrode; (b) SEM image of Au NPs/GO/CS modified electrode; (c) SEM image of Au NPs/GO/CS/L-GluOx modified electrode.

2.5. Determination of detection environment for L-Glu biosensor

The pH is an important influence factor on the performance of the biosensor since pH affects the enzyme activity. The pH range is 5–8.5: sodium acetate (pH 5.0–5.5), PBS (pH 6.0–8.0), and Tris–HCl buffer (pH 8.5) (Batra & Pundir, 2013). Temperature is another important influence factor, since the appropriate temperature is conducive to maintaining enzyme activity. The different temperatures (20–80 °C) of the buffer solution were studied at an interval of 10 °C. The effect of L-Glu concentration (0.2–1.4 mM) on L-Glu biosensor response was investigated. The conditions of differential pulse voltammetry are as follows: scanning range 0.2–0.6 V, potential increment 0.004 V, amplitude 0.05 V, pulse width 0.05 s, sampling width 0.0167 s, pulse period 0.2 s.

2.6. Detection of L-Glu in beef by the L-Glu biosensor

The beef hydrolysate was adjusted to pH 7.5 by adding 1 M KOH solution. Then 1 mL of a beef water solution was taken and diluted with a buffer solution. The three-electrode system was placed into the diluted beef hydrolysate for testing.

3. Results and discussion

3.1. Characterization of GO (graphene oxide)

Fig. 2a shows the infrared spectra of GO. Clearly, GO shows multiple characteristic peaks at 1041 cm^{-1} (stretching vibration of CH_3O—), 1224 cm^{-1} (stretching vibration of —CH—O—CH—), 1622 cm^{-1} (expansion vibration of —C═O), and 3417 cm^{-1} (telescopic vibration of —OH). The infrared spectra showed large amounts of carboxyl, carbonyl, hydroxyl, and other oxygen-containing groups in the structure of GO (Cao, Zhang, Chai, & Yuan, 2013; Xu, Bai, Lu, Li, & Shi, 2008). The XRD patterns of GO the peak at GO at $2\theta = 10.2°$, and $d = 0.87$ nm determined according to Bragg equation (Fig. 2b). The layer spacing of GO is larger compared with natural flake graphite, which is mainly attributed to the numerous carbonyl and hydroxyl groups between the layers of GO and to the entrance of water molecules into the interlayer of GO.

3.2. Electrochemical characterization of the Au electrode during modification

Fig. 3a and b shows the DPV (Differential pulse voltammetry) and CV (Cyclic voltammetry) curves respectively of the bare Au electrode, Au NPs/CS/Au electrode and L-GluOx/Au NPs/GO/CS/Au electrode. Clearly, the trends of the current peaks in the two modifications were the same. The L-GluOx/Au NPs/GO/CS/Au electrode showed a pair of obvious reversible redox peaks. The peak current decreased with the increase of the surface-modified material of the bare Au electrode, indicating Au NPs/GO/CS and L-GluOx were successfully surface-modified onto the of the Au electrode.

3.3. Characterization of the modified Au electrode by SEM

The bare Au electrode had smooth and clean surface, the Au NPs/GO/CS modifier was uniformly modified on the surface of the Au electrode, and the spherical Au NPs were evenly distributed in the modifier (Fig. 4). When the surface of the Au NPs/GO/CS/Au electrode was connected with L-GluOx, the surface became irregular and protuberant, which was conducive to electron transfer. Comparison with the electrochemical method showed L-GluOx was successfully modified to the surface of the Au NPs/GO/CS/Au electrode.

3.4. Performance of the L-Glu biosensor

The effects of pH and temperature on the performance of the L-Glu biosensor were studied (Fig. 5). At the optimum pH of L-GluOx (pH 7.5), the maximum response current of the L-Glu biosensor to L-Glu was 0.08 mA (Fig. 5a). With the increase of pH in the electrolyte solution, the oxidation peak current decreased. The reason was that when the pH of the electrolyte solution was low, the enzyme activity increased with the rise of pH, and the response current of the glutamate biosensor to glutamate also increased. When pH reached 7.5, the optimal pH of glutamate oxidase was achieved, and the response current of the glutamate biosensor to glutamate maximized. With further increase of pH, the higher pH inactivated glutamate oxidase, and the response current of the glutamate oxidase biosensor to glutamate decreased gradually. The peak current of glutamate oxidase at pH 5.5–6.5 did not change

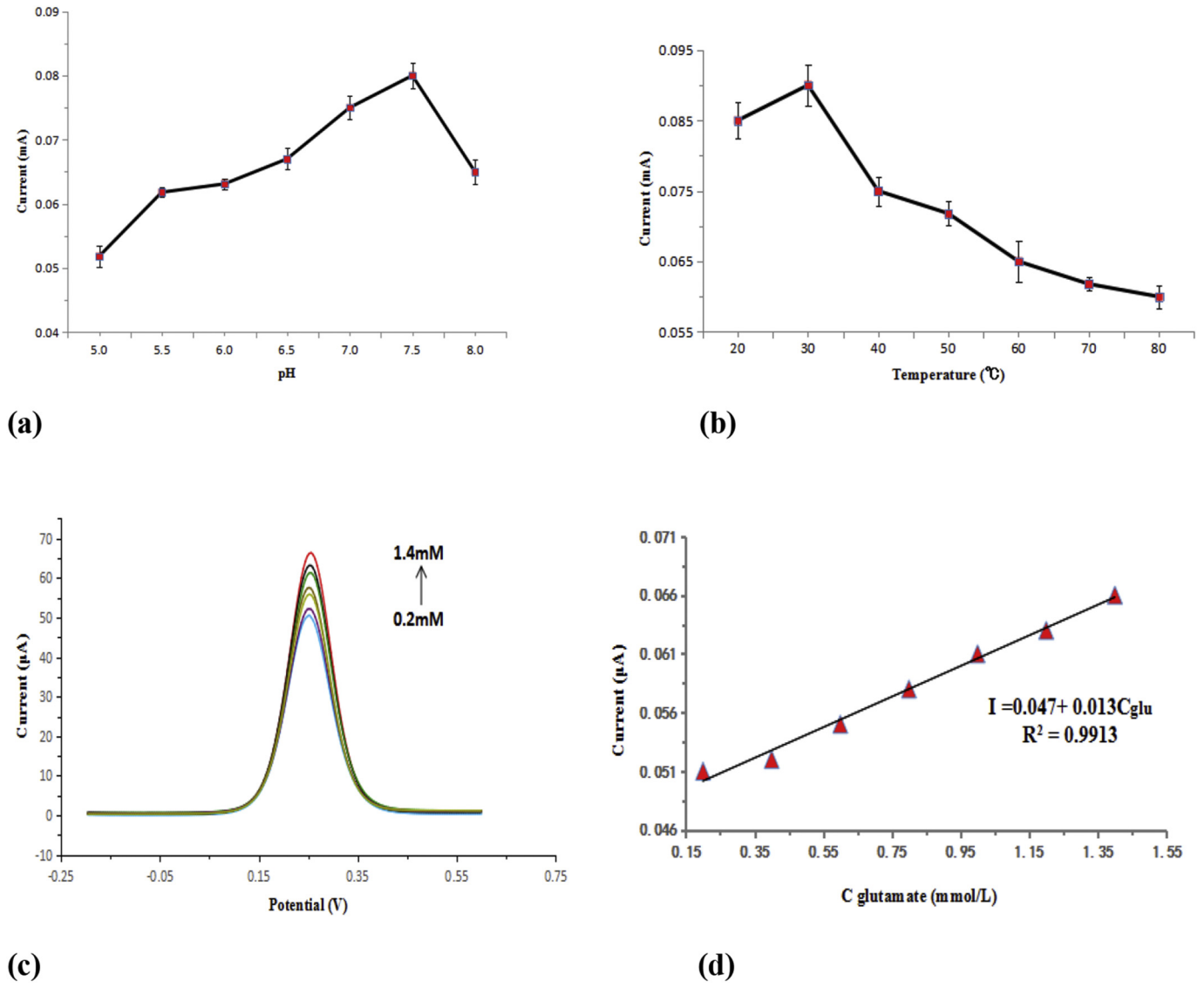

Fig. 5. (a) Effect of pH on catalytic performance of Au NPs/GO/CS/L-GluOx modified electrode. (b) Effect of temperature on catalytic performance of Au NPs/GO/CS/L-GluOx modified electrode. (c) The detection range of L-Glu by the biosensor. (d) The linear relationship between the concentration of L-Glu and the peak current.

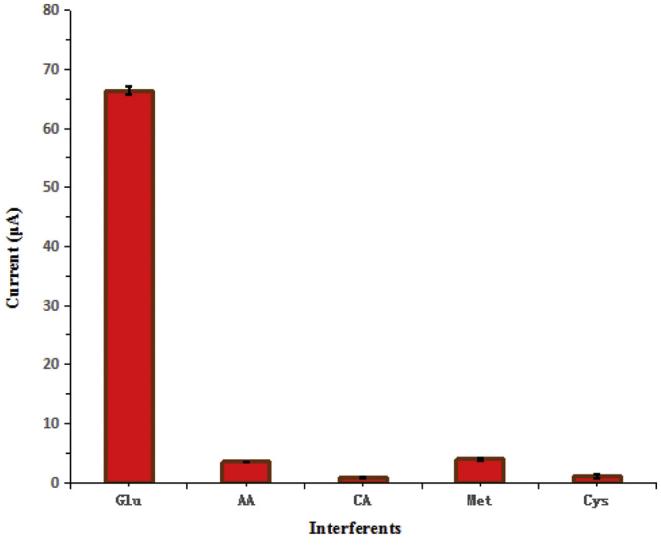

Fig. 6. Interference of glutamate biosensors by AA, CA, Met, and Cys.

significantly. Therefore, the optimal pH of the electrolyte solution was 7.5.

The temperature also significantly affected the catalytic performance of the enzyme-modified electrode. High temperature will lead to thermal denaturation of the enzyme, but low temperature will impact the catalytic effect of the enzyme. In addition, the effects of temperature on the free enzyme and the combined enzyme are also different. Clearly, the catalytic performance of the L-Glu biosensor was optimized at 30 ˚C, and the maximum oxidation peak current was 0.09 mA (Fig. 5b).

Under the condition of pH 7.5 and 30 ˚C, the L-Glu detection range by the biosensor was studied (Fig. 5c). It was found the L-Glu concentration and the peak current were linearly related (Fig. 5d). Clearly, the catalytic current of L-Glu was very significantly and linearly related with the L-Glu concentration within 0.2–1.4 mM (R^2 = 0.987, detection limit = 0.023 mM):

$$I = 0.047 + 0.013C_{L-glu} \quad (1)$$

where I is the peak current, $C_{L\text{-}glu}$ is the L-Glu concentration. Therefore, in the L-Glu detection, the L-Glu content in the sample can be calculated by the electrochemical response of the L-Glu biosensor to the target L-Glu.

Table 1
The results of L-Glu content in beef of different states were compared by two methods.

Samples	X_1: Amino acid analyzer (mmol/L)	X_2: Biosensor (mmol/L)	Residual absolue value (mmol/L)
C_{cooked}			
1	7.70	7.60	0.10
2	16.59	17.10	0.51
3	13.30	12.96	0.34
4	5.79	5.63	0.16
5	6.96	6.83	0.13
6	4.89	5.01	0.12
7	3.56	3.62	0.06
8	5.91	5.96	0.05
9	15.86	15.32	0.54
10	2.30	2.40	0.10
C_{raw}			
1	15.63	15.53	0.10
2	100.89	100.99	0.10
3	106.83	105.98	0.85
4	46.30	46.10	0.20
5	50.96	51.98	1.02
6	37.12	36.12	1.00
7	48.65	47.63	1.02
8	85.26	85.30	0.04
9	12.96	13.12	0.16
10	47.80	48.30	0.50

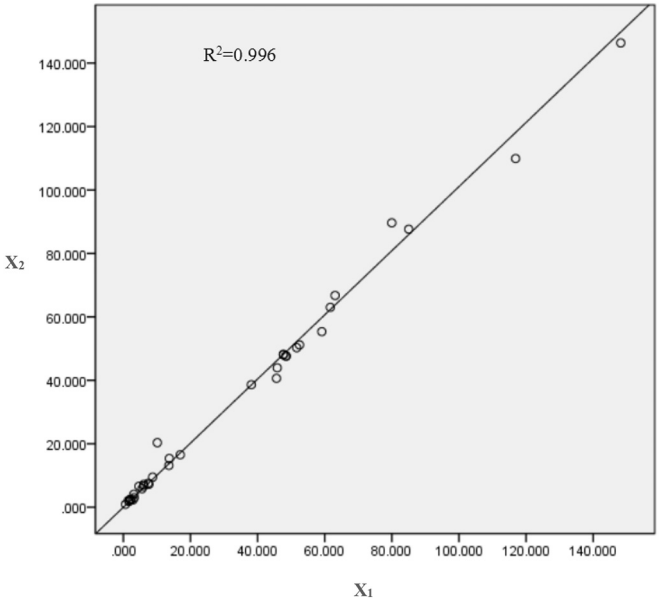

Fig. 7. Scatter diagram of measured values of biosensor and amino acid analyzer.

3.5. Anti-interference of the L-Glu biosensor

To explore the effects of other substances in the mixed system on the L-Glu biosensor, we added interfering substances (all 0.1 mM) including ascorbic acid (AA), citric acid (CA), L-methionine (Met) and L-cysteine (Cys) to the substrate solution containing L-Glu. In this process, the L-Glu biosensor was used to detect the mixed solution by the DPV method and record the change of the current.

The catalytic currents produced by AA, CA, Met, and Cys are 5.27%, 1.39%, 5.99%, and 1.60%, respectively (Fig. 6), indicating the L-Glu biosensor high good selectivity for L-Glu and strong anti-interference ability.

3.6. Repeatability and stability of the L-Glu biosensor

Under the same experimental conditions, the repeatability of the same L-Glu concentration was detected by using five biosensors, and the relative standard deviation was 5.4%. After the L-Glu biosensor was stored for 15 days at 4 °C, the stability was detected by measuring the same L-Glu concentration, which showed the current response was 92% of the original value. The weakening catalytic current may be due to the passivation of some enzymes. The above results indicate the L-Glu biosensor has high repeatability and stability.

3.7. Comparison of the L-Glu biosensor and the amino acid analyzer for L-Glu detection in beef

The glutamate content was detected by the glutamate biosensor according to the linear Eq. (1). As shown in Table 1, the detection results of the L-Glu biosensor are similar to those of the amino acid autoanalyzer. The maximum absolute residual value of the two detection methods is 1.02. The deviation of the the L-Glu biosensor is attributed to the presence of interfering amino acids in the beef hydrolysate. In addition, the L-Glu content in the cooked beef was higher than that of raw beef.

Pearson correlation analysis was conducted on SPSS 22.0, and 18 beef samples were tested in parallel for 3 times to build the model. The Pearson distribution scatter diagram was drawn (Fig. 7). The linear fit of the two methods is 0.996, which means that the data detected by the biosensor are highly correlated with the data detected by the amino acid analyzer.

3.8. Advantages of the L-Glu biosensor

Compared with the traditional amino acid analyzer, the L-Glu biosensor has the advantages of lower cost, shorter detection time, and more convenient sample pre-processing. The cost of the amino acid analyzer is much higher than those of the biosensor and the electrochemical workstation. Glutamate detection by the L-Glu biosensor can be completed within 5 min by collecting the response electrical signals from the electrochemical workstation, and the correlation coefficient between the biosensor and the amino acid analyzer is up to 0.996, indicating the biosensor has high accuracy.

4. Conclusions

The detection of L-Glu content in beef was tested. Three modification stages, including the bare gold electrode, the Au NPs/GO/CS modified electrode, and the Au NPs/GO/CS/L-GluOx modified electrode, were characterized by cyclic voltammetry and differential pulse voltammetry. The response currents of the two methods changed in the same trend. Au NPs/GO/CS and L-GluOx were successfully modified to the surface of the bare gold electrode. The L-Glu biosensor showed a good electrocatalysis response to L-Glu, with a detection range of 0.2–1.4 mM and a detection limit of 0.023 mM. The results of L-Glu detection by the L-Glu biosensor were similar to those by the amino acid analyzer. Meanwhile, the L-Glu content in cooked beef was higher than that of raw beef, indicating the taste of cooked beef was better and more pronounced than raw beef. The excellent performance of the L-Glu sensor benefited from the enzyme specificity. In summary, the L-Glu biosensor can effectively and accurately detect the L-Glu content in beef with a fast speed and high sensitivity.

Ethical approval

This article does not contain any studies with human or animal subjects.

Author statement

All authors have made substantial contributions to the conception or design of the work; or the acquisition, analysis, or interpretation of data for the work; and all authors have drafted the work or revised it critically for important intellectual content; and all authors have approved the final version to be published; and all authors agree to be accountable for all aspects of the work in ensuring that questions related to the accuracy or integrity of any part of the work are appropriately investigated and resolved.

Declaration of Competing Interest

Xiaodan Wang declares that she has no conflict of interest. Jinjiao Duan declares that she has no conflict of interest. Yingming Cai declares that she has no conflict of interest. Dengyong Liu declares that he has no conflict of interest. Xing Li declares that she has no conflict of interest. Yanli Dong declares that she has no conflict of interest. Feng Hu declares that she has no conflict of interest.

Acknowledgments

This study was financially supported by the Jilin Provincial Natural Science Foundation of China (No.20160101274JC).

References

Acebal, C. C., Lista, A. G., & Fernández Band, B. S. (2008). Simultaneous determination of flavor enhancers in stock cube samples by using spectrophotometric data and multivariate calibration. *Food Chemistry, 106*(2), 811–815.

Ali, A., Hwang, E. Y., Choo, J., & Dong, W. L. (2017). Nanoscale graphene oxide-induced metallic nanoparticle clustering for surface-enhanced raman scattering-based IgG detection. *Sensors and Actuators B: Chemical, 255*, 183–192.

Basu, A. K., Chattopadhyay, P., Roychudhuri, U., & Chakraborty, R. (2006). Development of biosensor based on immobilized L-glutamate oxidase for determination of monosodium glutamate in food. *Indian Journal of Experimental Biology, 44*(5), 392–398.

Batra, B., & Pundir, C. S. (2013). An amperometric glutamate biosensor based on immobilization of glutamate oxidase onto carboxylated multiwalled carbon nanotubes/gold nanoparticles/chitosan composite film modified au electrode. *Biosensors & Bioelectronics, 47*(47C), 496–501.

Batra, B., Yadav, M., & Pundir, C. S. (2016). L-Glutamate biosensor based on L-glutamate oxidase immobilized onto ZnO nanorods/polypyrrole modified pencil graphite electrode. *Biochemical Engineering Journal, 105*, 428–436.

Buck, K., Voehringer, P., & Ferger, B. (2009). Rapid analysis of gaba and glutamate in microdialysis samples using high performance liquid chromatography and tandem mass spectrometry. *Journal of Neuroscience Methods, 182*(1), 78–84.

Cao, S., Mishra, R., Pilla, S., Tripathi, S., Pandey, M. K., Shah, G., ... Tiwari, A. (2010). Novel chitosan/gold-MPA nanocomposite for sequence-specific oligonucleotide detection. *Carbohydrate Polymers, 82*(1), 189–194.

Cao, S., Zhang, L., Chai, Y., & Yuan, R. (2013). Electrochemistry of cholesterol biosensor based on a novel pt-pd bimetallic nanoparticle decorated graphene catalyst. *Talanta, 109*(109), 167–172.

Chuanrui, C., Yue, G., Peining, C., & Huisheng, P. (2020). Recent advances of tissue-interfaced chemical biosensors. *Journal of Materials Chemistry B, 8*(3), 416–425.

Clarke, G., O'Mahony, S., Malone, G., & Dinan, T. G. (2007). An isocratic high performance liquid chromatography method for the determination of gaba and glutamate in discrete regions of the rodent brain. *Journal of Neuroscience Methods, 160*(2), 223–230.

Denuziere, A., Ferrier, D., Damour, O., & Domard, A. (1998). Chitosan-chondroitin sulfate and chitosan-hyaluronate polyelectrolyte complexes: Biological properties. *Biomaterials, 19*(14), 1275–1285.

Elancheziyan, M., Manoj, D., Saravanakumar, D., Thenmozhi, K., & Senthilkumar, S. (2017). Amperometric sensing of catechol using a glassy carbon electrode modified with ferrocene covalently immobilized on graphene oxide. *Microchimica Acta,* 1–8.

Han, Y. X., Wang, X. D., Cai, Y. X., Li, Z. Y., Zhao, L., Wang, H. M., ... Zhu, L. T. (2017). Sensor-array-based evaluation and grading of beef taste quality. *Meat Science, 129*, 38–42.

Hayashi, T., Yamaguchi, K., & Konosu, S. (1981). Sensory analysis of taste-active components in the extract of boiled snow crab meat. *Journal of Food Science, 46*(2), 479–483.

Hocquette, J. F., Botreau, R., Picard, B., Jacquet, A., Pethick, D. W., & Scollan, N. D. (2012). Opportunities for predicting and manipulating beef quality. *Meat Science, 92*(3), 197–209.

Hughes, G., Pemberton, R. M., Fielden, P. R., & Hart, J. P. (2015). Development of a novel reagentless, screen-printed amperometric biosensor based on glutamate dehydrogenase and NAD^+, integrated with multi-walled carbon nanotubes for the determination of glutamate in food and clinical applications. *Sensors and Actuators B: Chemical, 216*, 614–621.

Khampha, W., Meevootisom, V., & Wiyakrutta, S. (2004). Spectrophotometric enzymatic cycling method using L-glutamate dehydrogenase and D-phenylglycine aminotransferase for determination of L-glutamate in foods. *Analytica Chimica Acta, 520*(1–2), 133–139.

Kitikul, J., Satienperakul, S., Preechaworapun, A., Pookmanee, P., & Tangkuaram, T. (2017). A simple flow amperometric electrochemical biosensor based on chitosan scaffolds and gold nanowires modified on a glassy carbon electrode for detection of glutamate in food products. *Electroanalysis, 29*(1), 264–271.

Kuila, T., Bose, S., Khanra, P., Mishra, A. K., Kim, N. H., & Lee, J. H. (2011). Recent advances in graphene-based biosensors. *Biosensors & Bioelectronics, 26*(12), 4637–4648.

Omanovic-Miklicanin, E., & Valzacchi, S. (2017). Development of new chemiluminescence biosensors for determination of biogenic amines in meat. *Food Chemistry, 235*, 98–103.

Scollan, N. D., Dannenberger, D., Nuernberg, K., Richardson, I., MacKintosh, S., Hocquette, J. F., & Moloney, A. P. (2014). Enhancing the nutritional and health value of beef lipids and their relationship with meat quality. *Meat Science, 97*(3), 384–394.

Shen, J., & Burgess, D. J. (2018). Advances in drug delivery related biosensors and medical devices. *International Journal of Pharmaceutics, 544*(2), 307–308.

Shi, W., & Ma, Z. (2010). Amperometric glucose biosensor based on a triangular silver nanoprisms/chitosan composite film as immobilization matrix. *Biosensors & Bioelectronics, 26*(3), 1098–1103.

Song, J., Xu, L., Zhou, C., Xing, R., Dai, Q., Liu, D., & Song, H. (2013). Synthesis of graphene oxide based CuO nanoparticles composite electrode for highly enhanced nonenzymatic glucose detection. *ACS Applied Materials & Interfaces, 5*, 12928–12934.

Sorlier, P., Denuzière, A., Viton, C., & Domard, A. (2001). Relation between the degree of acetylation and the electrostatic properties of chitin and chitosan. *Biomacromolecules, 2*(3), 765–772.

Stankovich, S., Dikin, D. A., Piner, R. D., Kohlhaas, K. A., Kleinhammes, A., Jia, Y., ... Ruoff, R. S. (2007). Synthesis of graphene-based nanosheets via chemical reduction of exfoliated graphite oxide. *Carbon, 45*(7), 1558–1565.

Stredansky, M., Redivo, L., Magdolen, P., Stredansky, A., & Navarini, L. (2018). Rapid sucrose monitoring in green coffee samples using multienzymatic biosensor. *Food Chemistry, 254*, 8–12.

Tadayuki, T., & Kiyoshi, M. (2005). Sequential fluorometric quantification of γ-aminobutyrate and L-glutamate using a single line flow-injection system with immobilized-enzyme reactors. *Analytica Chimica Acta, 546*(2), 154–160.

Tang, L., Zhu, Y., Xu, L., Yang, X., & Li, C. (2007). Amperometric glutamate biosensor based on self-assembling glutamate dehydrogenase and dendrimer-encapsulated platinum nanoparticles onto carbon nanotubes. *Talanta, 73*, 438–443.

Upadhyay, S., Rao, G. R., Sharma, M. K., Bhattacharya, B. K., Rao, V. K., & Vijayaraghavan, R. (2009). Immobilization of acetylcholineesterase-choline oxidase on a gold-platinum bimetallic nanoparticles modified glassy carbon electrode for the sensitive detection of organophosphate pesticides, carbamates and nerve agents. *Biosensors & Bioelectronics, 25*(4), 832–838.

Xu, Y., Bai, H., Lu, G., Li, C., & Shi, G. (2008). Flexible graphene films via the filtration of water-soluble noncovalent functionalized graphene sheets. *Journal of the American Chemical Society, 130*(18), 5856.

Zhang, S. Y., Zhang, C. Y., Qian, Y., Xing, L. J., Kang, D. C., Khan, I. A., ... Zhou, G. H. (2017). Effect of flavourzyme on proteolysis, antioxidant activity and sensory qualities of Cantonese bacon. *Food Chemistry, 237*, 779–785.